Photoinduced Proton Transfer and Rotational Motion of 1-Hydroxy-2-acetonaphthone in the S_1 State: A Theoretical Insight into Its Photophysics

Juan Angel Organero,[†,‡] Miquel Moreno,[§] Lucía Santos,[‡] José Maria Lluch,[§] and Abderrazzak Douhal*[,†]

Departamento de Química Física, Facultad de Ciencias del Medio Ambiente, Campus Tecnológico de Toledo, Avenida Carlos III, S.N., Universidad de Castilla-La Mancha, 45071 Toledo, Spain, Departamento de Química Física, Facultad de Ciencias, Universidad de Castilla-La Mancha, 13071 Ciudad Real, Spain, and Departament de Química, Facultat de Ciències, Universitat Autònoma de Barcelona, 08193 Bellaterra, Barcelona, Spain

Received: May 3, 2000

The internal rotational motion, the intramolecular proton-transfer reaction, and the subsequent internal twisting process of 1-hydroxy-2-acetonaphthone (HAN) are studied in the first singlet excited electronic state (S_1) using the ab initio electronic-structure method at the CIS/6-31G** level. The calculations show a multiple-well potential-energy surface (PES) with a low energy barrier (5.49 kcal/mol) between the excited OH···OC enol form (E*, the most stable structure at the ground state) and its keto tautomer (K*, result of intramolecular proton-transfer reaction). An internal rotation with activation energy of 7.53 kcal/mol in the produced K* may give a more stable twisted rotamer KR*. The energy of this structure is 6.23 kcal/mol lower than that of E*. The involvement of a twisting motion in the tautomer explains the reported structured fluorescence band, the low quantum yield, and short emission lifetime. The existence of energy barriers in the PES accords with the dependence of its emission spectroscopy and dynamics on the nature of the transferred isotope (H/D) and on the excess energy of excitation. Frequency modes analysis shows that in-plane and out-of-plane motions of the H-bonded chelate ring of E* will play a crucial role in the proton-transfer dynamics and spectroscopy. These theoretical results are in full agreement with previous experimental observations in the gas phase (Douhal, A.; et al. *Chem. Phys.* **1993**, *178*, 493. Lu, C.; et al. *Chem. Phys. Lett*. **1999**, *310*, 103) and in solution (Tobita, S.; et al. *J. Phys. Chem. A.* **1998**, *102*, 5206). However, they contrast with the conclusion of Catalán et al. stating the absence of proton transfer in the S_1 state and the presence of a single minimum at the S_0 state (Catalán, J.; et al. *J. Am. Chem. Soc*. **1993**, *115*, 4321; *Chem. Phys. Lett.* **1997**, *269*, 151). Moreover, the ER−OH and ER−CO isomers having rotated the OH and C═O groups, are found at 13.95 and 17.36 kcal/mol above the E* structure, respectively. As a result of the pseudoaromaticity provided by the H-bonded chelate ring in the enol form, the electronic excitation induces in this one a stabilization of ∼2 kcal/mol with respect to ER−OH and ER−CO rotamers.

1. Introduction

The field of the photoinduced proton-transfer process, despite the great efforts devoted since Weller,[1] still poses challenges both theoretically and experimentally. This is mainly due to the complexity of its physical (e.g., quantum nature) and chemical (H-bond breaking and making and subsequent nuclear rearrangement with inversion in the thermodynamic stability) nature. Nevertheless, the use of modern techniques allowing spectrally and time-resolved experiments together with those of ab initio calculations have allowed a direct observation of the parameters in few systems that are relevant to the mapping of the potential-energy surface (PES).[2−22] It is well-known that the partners in a H-bond might adopt several conformations, giving birth to other structures with different reactivity and dynamics. For instance, methyl salicylate (MS) is one of the most studied organic molecules showing at least two stable isomers with a striking difference in stability and dynamics.[8−13] Herek et al. have shown that the first singlet excited electronic state (S_1) dynamics of the proton motion in the more populated structure of MS at S_0 is in the femtosecond time scale.[13] The less stable conformer of MS does not show such an internal reaction.[10,11] Acuña and co-workers have shown that salicylamide, a molecule that belongs to the MS family and which shows a proton transfer at S_1, exhibits an efficient lasing action in solution.[14] Therefore, studying the stability (energy domain) and structure (space domain) of possible conformers due to the breaking and making of a H-bond is of great interest from the point of view of molecular science and technological applications.[1−22]

A few years ago, we reported on 1-hydroxy-2-acetonaphthone (HAN) (Scheme 1) in jet-cooled molecular beam.[20] The fluorescence data indicated a single conformer populated at the S_0 state and the occurrence of an excited-state intramolecular proton-transfer (ESIPT) reaction at the S_1 state. We observed an unusual dual fluorescence and a striking isotope (OH/OD) effect on the emission spectrum under molecular beam conditions. On the basis of the structured and abnormally shifted emission band of the tautomer, we proposed that the ground-state potential energy surface (PES) might contain additional minima. Femtosecond[21] as well as nanosecond−microsecond[22]

* Corresponding author. Tel: +34-925-265717. Fax: +34-925-268840. E-mail: adouhal@amb-to.uclm.es.
† Campus Tecnológico de Toledo, Universidad de Castilla-La Mancha.
‡ Universidad de Castilla-La Mancha, Ciudad Real.
§ Universitat Autònoma de Barcelona.

10.1021/jp001671m CCC: $19.00
Published on Web 08/19/2000

Scheme 1:[a] **Molecular Structures of Enol (E*), Keto (K*), Keto Rotamer (KR*) and Rotational Isomers (ER−OH* and ER−CO*) of 1-Hydroxy-2-acenaphthone (HAN) Expected at the S_1 State**

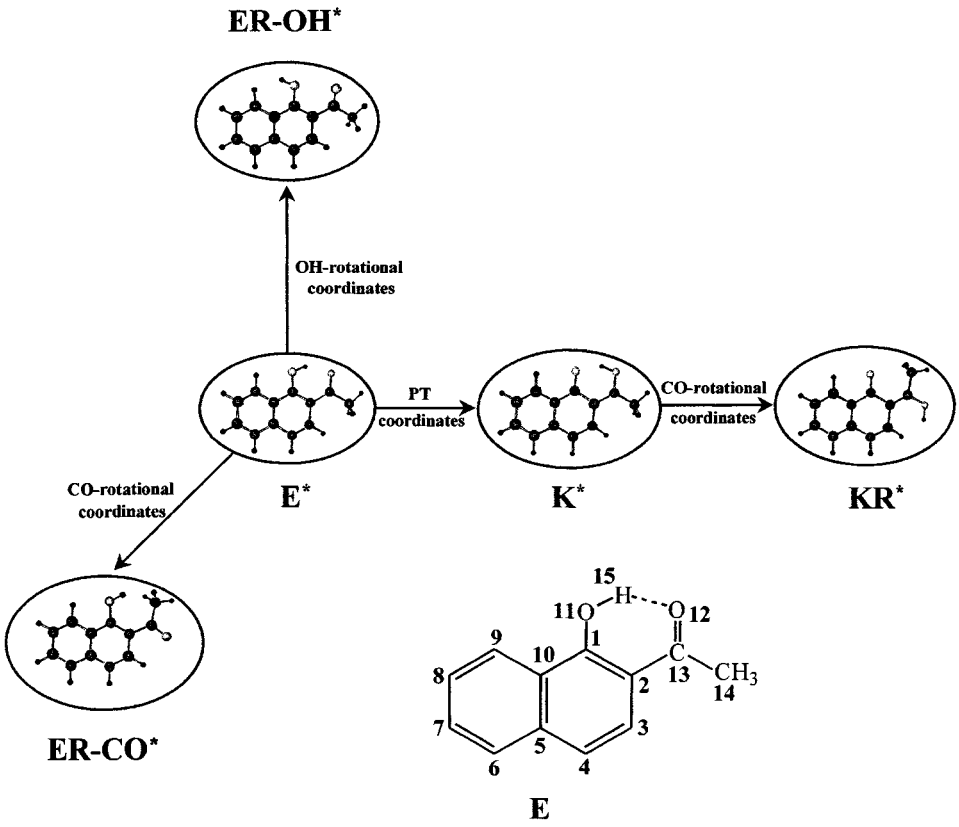

[a] The arrows are for proton (or hydrogen atom) or twisting motion which connect the different species along proton and/or rotational coordinates. For clarity, the molecular structure of E including the numbering of the atoms is shown.

measurements have recently elucidated the fast and slow dynamics of HAN in gas and in condensed phases, respectively. Cheng and co-workers measured the rate of proton transfer and relaxation pathways of the excited produced tautomer and found the existence of a barrier for the transfer.[21] Tobita et al. have suggested that the ESIPT reaction in HAN is followed by a structural change to produce a metastable isomer.[22] Both of the above time-resolved reports agree with our previous assignment based on molecular beam data.[20] However, Catalán et al. reports based on steady-state and S_0 calculations contrast with these works and conclude that HAN cannot undergo an ESIPT reaction.[23,24]

In a recent contribution, we reported on the S_0 state structures of HAN in both gas and bulk media.[25] We found that the most stable structure of HAN is that having an internal H-bond (structure E in the Scheme 1). Those with different conformations of the OH or $CO(CH_3)$ groups or result of proton transfer and twisting motion might be formed through an excitation of the E structure or through H-bonding interactions with the solvent. Here, we continue our efforts in this field by studying, from the point of view of quantum chemistry, the structures of HAN related to the proton-transfer reaction and to the rotational motion at the S_1 state (Scheme 1). The theoretical results are in full agreement with the experimental observation in gas as well as in condensed phases showing the occurrence of both proton transfer and rotational motion in S_1.[20−22,26] However, our findings again contrast with those of Catalán et al.[23,24] The difference comes from the fact that the interpretation of these authors is based on limited one-coordinate calculations carried out at the S_0 state. As in previous reports in this field, we are dealing with the S_1 state structures using a full geometry optimization for both local minima and the involved transition states.[15,16,27,28]

2. Theoretical Details

Ab initio calculations have been performed within the Gaussian 94 and 98 series of programs.[29,30] The S_0 state has been studied through the restricted Hartree−Fock method (RHF), whereas a CI all-single-excitations with a spin-restricted Hartree−Fock reference ground state (CIS) has been used for the excited S_1 state.[31] The energies of the ground-state S_0 have been recalculated through the Möller−Plesset perturbation theory up to second order (MP2).[32]

All calculations have been done with the split-valence 6-31G-(d,p) basis set, which includes a set of d polarization functions on heavy atoms and p polarization functions on hydrogens.[33] Full geometry optimization and direct location of stationary points (minima and transition states) have been carried out by means of the Schlegel gradient optimization algorithm by using redundant internal coordinates as implemented in the Gaussian 94 and 98 packages.[29,30] Diagonalization of the energy second-derivative matrix has been carried out to disclose the nature of each stationary point: no negative eigenvalues indicate a minimum, whereas one negative eigenvalue identifies a transition state. This calculation also provides the harmonic vibrational frequencies of the minimum energy structures. As suggested by several authors,[34] the calculated Hartree−Fock (or CIS) frequencies have been scaled by a factor of 0.9 prior to be compared with the experimental data.

3. Results and Discussion

3.1. Ground-State Structures. We briefly describe the situation at the S_0 state, which has been reported in a recent work.[25] The most stable structure has an intramolecular H-bond

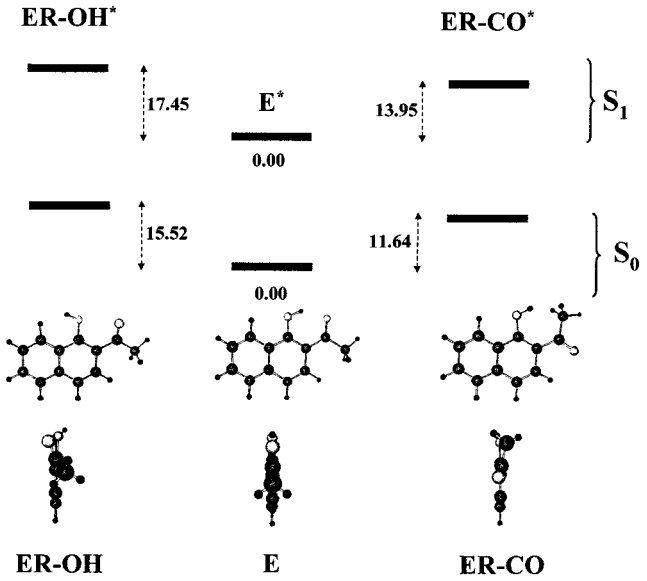

Figure 1. Schematic energy diagram for the S_0 and S_1 states of E, ER−CO, and ER−OH structures of HAN. Energies relative to the enol structure are given in kcal/mol. The transition energy between the S_0 and S_1 states is not indicated.

between the OH and the CO groups (E structure in Scheme 1 and Figure 1). At about 12.0 and 15.5 kcal/mol from this structure, OH and CO groups might rotate, giving birth to the OH and CO isomers where the intramolecular H-bond is absent. To induce a proton-transfer reaction in E and a possible subsequent twisting motion of the resulted protonated carbonyl group, an energy of 59.13 kcal/mol is needed to overcome the barrier. The produced structure (KR, Figure 2) is found at 22.09 kcal/mol above E. Figure 2A schematically represents the energy profile of the obtained stationary points for E, KR, and the involved transition state (TS) in S_0. Because the reaction paths for proton transfer and twisting motion are quite different, the whole reaction from E to the final rotamer of the keto type cannot be represented using a one-dimensional coordinate. Thus, the line connecting the stationary points drawn in Figure 2A only indicates the connection between minima in the potential energy hypersurface through the corresponding transition state. For the sake of clarity, we give for each structure the dihedral angle (rotational coordinate) between the plane formed by the transferring H-atom and the two oxygen atoms between which the chemical event occurs and that of the naphthalene frame.

Comparison of geometry for E and KR, depicted in Figure 3A, shows that the C_2-C_{13} bond has been rotated by 180°. The C_1-O_{11} and the C_2-C_{13} bond distances are shorter in KR by 0.12 and 0.11 Å, respectively. Correspondingly, in KR the C_1-C_2 and $C_{13}=O_{12}$ (carbonyl) bond distances are elongated by 0.10 and 0.12 Å, respectively. As for the rest of the C−C bond distances of the naphthalene part, they adopt an alternate long−short pattern in KR. This loss of aromaticity explains the lack of stability of the tautomer and the high energy of the KR structure. The TS connecting both minima with a dihedral angle of 93° involves an energy barrier of 59.13 kcal/mol. Considering this high energy, we suggest that at the S_0 state the only populated state will correspond to that of E. However, as discussed elsewhere[25] and elucidated below, KR might be populated through the relaxation of produced structures at S_1 obtained upon photoexcitation of E.

3.2. Excited-State Structures. We first consider the result of the calculation dealing with the OH and C=O rotational motion in excited E to produce ER−OH and ER−CO, respectively (Scheme 1). An asterisk is used to indicate the excited electronic state. The calculations show that E* is the most stable rotamer at S_1 as found for the S_0 state (Figure 1). Indeed, the energy difference between the rotamers E* and ER−CO* and ER−OH* increases by about 2 kcal/mol with respect to the values found in the S_0 state. This relative stabilization of E* is due to extended p-conjugation provided by the pseudo-aromaticity of the H-bonded chelate ring in this structure. Thus, the electronic excitation increases the strength of the H-bond in HAN. This accords well with the experimental evidence of the strengthening of the H-bond in excited HAN in the gas phase.[20] Similar findings have been observed in other systems.[35−38] From the point of view of geometry, ER−CO* and ER−OH* isomers did not experience important change when compared to the situation at S_0. However, the E* structure suffers changes in bond distances relevant to the proton-transfer reaction.

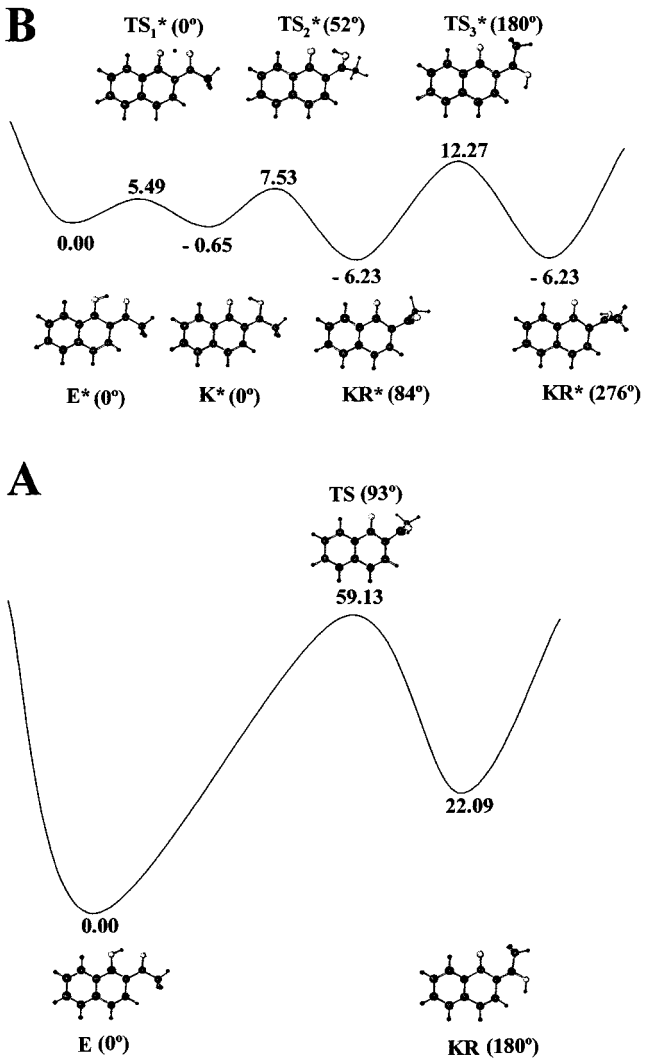

Figure 2. Schematic energy profile including the involved structures for proton transfer and twisting motion of HAN in both the (A) S_0 and (B) S_1 states. Energies relative to E or to E* are given in kcal/mol. We indicate between brackets the angle of the acetyl rotation around C_2-C_{13} bond.

Figure 2B is a schematic energy profile for the stationary points located in the S_1 state related to the proton-transfer reaction: the minima E*, K*, and KR* and the transition states TS_1*, TS_2* and TS_3*. The figure also shows the structure with the relevant rotational angle of the carbonyl group. Let us first consider the proton-transfer process. K* (the excited tautomer

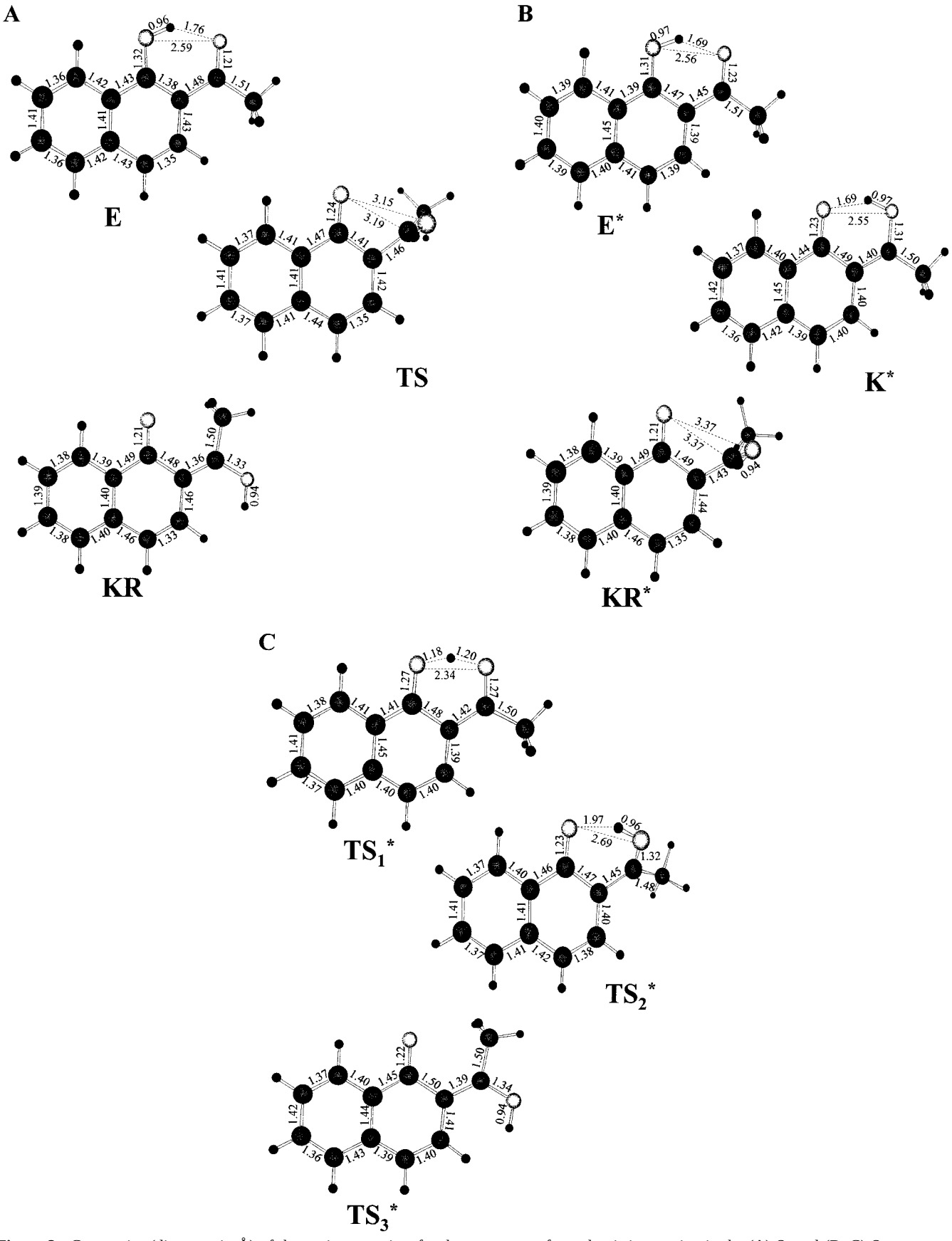

Figure 3. Geometries (distances in Å) of the stationary points for the proton transfer and twisting motion in the (A) S_0 and (B, C) S_1 states.

of E*), with a planar conformation, is almost isoenergetic to E* (the energy difference between both structures is 0.65 kcal/mol). CIS/3-21G calculations by Tobita et al. have found 2.35 kcal/mol as energy difference between E* and K*.[22] The transition state (TS_1*) connecting E* and K* is planar and involves an energy barrier of only 5.49 kcal/mol. This low energy barrier and the comparable energies of E* and of K* are in full agreement with the experimental observations

showing the existence of an energy barrier and a dual emission of HAN in the gas phase and the establishment of an equilibrium between E* and K*.[20] These findings also agree with the conclusion of the femtosecond experiment in the gas phase at room-temperature carried out by Cheng and co-workers.[21] From the point of view of bond distances, a comparison of E* and K* (Figure 3B) shows that the C−C bond distances of the naphthalene rings, which reflects in space the aromaticity of the electronic structure, suffer only minor variations. Thus, it seems that in S_1 there is not an important loss of aromaticity when the proton transfer takes place in E* to produce K*. The $O_{11}-O_{12}$ distance, which is one of the most relevant distances in the proton-transfer process, shows a compression of 0.22 Å, followed by an elongation of 0.21 Å, along the E* → TS$_1$* → K* processes (Figure 3B,C). Once the E* → K* reaction has taken place, a conformational change of K* along a rotational coordinate of the PES may occur to produce the rotamer KR*. This process has been found to be very favorable in S_0, where K converts easily to KR, as said above. A rotation around the C_2-C_{13} bond of K* leads to a stable KR* structure having an energy of 5.58 and 6.23 kcal/mol below K* and E*, respectively (Figure 2B). KR* is now the most stable structure in S_1. Interestingly, it does not correspond to a planar structure as it was the case for the analogous KR obtained in S_0. Indeed, its geometry shows the protonated acetyl group almost perpendicular (84°) to the plane defined by the naphthalene ring. A transition state (TS$_2$*) connecting K* to KR* has also been located with an energy of 7.53 kcal/mol relative to E* (that is, 8.18 kcal/mol relative to K*) and with a rotational angle of 52° for the protonated acetyl group. By continuing the rotation around the C_2-C_{13} bond, another transition state (TS$_3$*) is found at 180° of rotation with an energy of 12.27 kcal/mol above E*. TS$_3$* connects KR* with an equivalent structure (labeled also KR* in Figure 2B) corresponding to a total rotation of 276° around the C_2-C_{13} bond. This transition state involves the highest energy barrier in S_1.

To further analyze the energy profile at S_1 and its relevance to the spectroscopy and dynamics of HAN, we will take into account the changes in bond distances (Figure 3B,C), energy barriers (Figure 2B), and the charge redistribution with the evolution of the structures along the chemical and photochemical processes. Our interest will be focused on three relevant processes: (1) the effect of electronic excitation of E, which gives birth to the driving force behind the proton-transfer reaction, that is, *a fast electronic redistribution and a vibrational coherence of the elementary modes that modulate the transfer*;[7] (2) the relative stability of E*, K*, and KR*, the minimum energy structures in S_1; and (3) the relaxation of these excited structures to the S_0 state.

3.2.1. Effect of Electronic Excitation. Due to the electronic excitation, and as far as proton transfer is considered, the behavior of HAN in S_1 is completely different from that in S_0. As the CIS calculations indicate, the excited electronic state mainly comes from an HOMO−LUMO excitation. Figure 4 shows these two orbitals for the E*, K*, and KR* structures. Both orbitals are of p type so that the $S_0 \rightarrow S_1$ excitation can be labeled as a p−p* transition. In agreement with the report of Tobita and co-workers,[22] the new electronic distribution induces changes in E* (Figure 3). For example, upon excitation the C_1-C_2 bond distance enlarges 0.09 Å, whereas the $O_{12}-H_{15}$ bond distance diminishes 0.07 Å. The $O_{11}-O_{12}$ distance is also shortened by 0.03 Å in E*. On the basis of OH/OD IR frequencies of HAN and on the isotope effect on the O−O transition in gas phase, we have previously estimated the

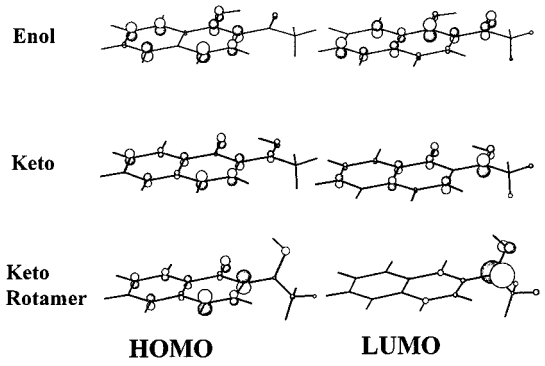

Figure 4. Shape of the HOMO and LUMO involved in the electronic excitation $S_0 \rightarrow S_1$ for enol, keto tautomer, and keto rotamer structures.

O···O distance as 2.6 Å.[20] Our present calculations showed that this distance is 2.56 Å. The photoinduced changes in bond distances can be correlated with the change in bonding character of the p orbitals (Figure 4) and with the Mulliken charges, as we reported in other systems.[15,27] Considering the HF and CIS data for S_0 and S_1, respectively, the electronic excitation induces a charge redistribution in the H-bonded chelate ring. For example, C_1 and C_2 atoms decrease their electronic density by 0.04 and 0.05 e, respectively. In a parallel way, the O_{11} and O_{12} atoms have gained an electronic density of 0.01 and 0.02 e, respectively. Furthermore, the charge analysis reveals an important electronic charge increment (0.07 e) in the CO(CH$_3$) fragment upon excitation. This increase can easily be explained by looking at Figure 4. The LUMO shows a larger contribution of the atoms in the CO(CH$_3$) fragment (mainly C_{13}) than the HOMO. This reorganization of charges, which is the fundamental basis for the increase in basicity (pK_b) of the carbonyl group and the decrease in acidity (pK_a) of the OH one upon electronic excitation, is the driving force for the H-bond breaking and making in excited HAN.

Moreover, analysis of the theoretical vibrational frequencies for the enol structure in S_1 reveals the presence of active vibrations at 325 and 381 cm^{-1} (in-plane) and 380 cm^{-1} (out-of-plane), which correspond to bending deformations of the H-bonded ring. The in-plane motion of the carbonyl group, with a frequency of 539 cm^{-1}, is predicted to have a very high IR intensity. These values are to be compared with those observed in the excitation spectrum of the dispersed fluorescence under jet-cooled molecular beam conditions.[20] The spectrum shows intense bands at 307, 365 and 370 cm^{-1} from the origin. Other bands assigned to out-of-plane motion (203 cm^{-1}) of the C−O−H group and in-plane bending mode (677 cm^{-1}) of the C═O group have also been observed in the spectrum.[20] They should be correlated with the corresponding ab initio calculated frequencies of 189 and 539 cm^{-1}, respectively. The bending of this part in the chelate ring induces a variation of the O···O distance and therefore can be considered as an active mode in the proton-transfer dynamics of HAN.[20] Similar observations have been reported in methyl salicylate.[9] The changes in acidity/basicity character of the involved partners is governed by the fast electronic redistribution and must occur in the subpicosecond time scale.[1−7] Therefore, the time scale for proton transfer in HAN will be mainly dictated by the in-plane and out-of-plane motions of the H-bonded chelate ring. Sobolewski and Domcke have suggested the importance of the out-of-plane bending motion of the O−H in the relaxation pathways of a related proton-transfer system at S_1.[19] Our calculations show that this mode has a frequency of 822 cm^{-1} and a very high

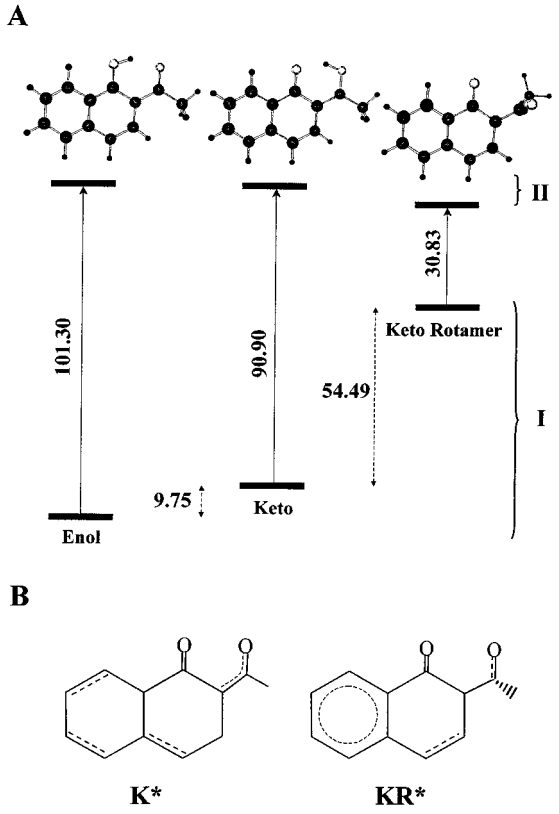

Figure 5. (A) Energy diagram (kcal/mol) of fully optimized enol, keto, and keto rotamer structures in S_1 state without (I, ground state) and with (II, excited state) electronic excitation energy indicated along the solid line arrows. (B) Lewis structures of K* and KR* showing a greater π-conjugation in KR* due to the fused phenyl ring.

activity, a fact that would account for the observation of an efficient radiationless channel operating beyond ca. 900 cm^{-1} of excess vibrational energy in jet-cooled molecular beam conditions.[20]

3.2.2. Stability of the Excited Structures. A significant result drawn in the energy profile of S_1 is the great stability of the nonplanar KR* keto rotamer (Figure 2B). To further analyze this point we invoke the shape of the HOMO and LUMO and their variation upon rotation around the C_2-C_{13} bond (Figure 4). In K*, the orbitals are qualitatively almost similar to those of E*. The HOMO for E*, K*, and KR* are also similar. However, the LUMO for KR* is quite different from that of the rest of the orbitals, as it is no longer delocalized around the whole molecular system. Indeed, it is almost totally localized in the $C(CH_3)O$ fragment. This orbital may be classified as a $C_{13}-O_{12}$ *localized* p antibonding orbital. Because this bond in KR* lies in a perpendicular plane with respect to the p system of the naphthalene frame, it does not mix with it. It appears then that the absence of mixing is greatly stabilizing this orbital.

To better understand this point, we have analyzed the energies of the three minima (E*, K*, and KR*) found in S_1. Figure 5A shows an energy decomposition diagram corresponding to the optimized geometries of S_1. The total electronic energies of the three minima in S_1 are split into two terms: the energy of the ground state (S_0) electronic configuration plus the electronic excitation energy. From Figure 5A it is clear that the greater stability of K* and KR* as compared with E* comes from a lower excitation energy term. This term is dramatically reduced in the KR* structure. In fact, the total relative energies, shown in Figure 2B, are the result of the sum of the two quantities given in Figure 5A. Without taking into account the electronic excitation energies, E* would be the more stable structure and KR* would possess a very high energy caused by the breaking of the H-bond and the rotation of the protonated acetyl group. Thus, once the H-bond has been broken, the only source that may favor a planar structure for the rotamer, is the p-conjugation of the C═O bond with the aromatic system. Because of the rotation, this conjugation is no longer present in KR*. However, in the electronic excited state the energy needed to break the H-bond is largely compensated by the much lower excitation energy observed for the KR* structure. This indicates a great stabilization upon rotation of the LUMO, the orbital to be occupied in the single electronic excitation. It is noteworthy that, without the electronic excitation term, the relative energy of KR* with respect to E* is quite similar to the value found for the transition state corresponding to the proton-transfer and rotation in the ground electronic state (TS). This is an unsurprising result given the very similar geometries of KR* and TS, as can be seen in Figure 3.

A simple picture based on the conjugation of a p-system through the single bond/double bond character alternation can be used to explain the great stability of KR* relative to K*. Taking into account the values of the calculated distances (Figure 3B), the Lewis structures of K* and KR* can be drawn as shown in Figure 5B. It is clear that the p-conjugation involving the left-fused phenyl ring in the KR* structure leads to a greater stability when compared to that of K*. Therefore, the lack of conjugation of the protonated acetyl group in KR* is greatly compensated by the high conjugation of the fused phenyl ring in the rotamer. Interestingly, this opens the possibility to control the relative stability of KR* to that of K* by selectively adding an electron donor or acceptor group in this ring.

3.2.3. Relaxation from the Excited to the Ground Electronic State. Relevant findings for the spectroscopy and dynamics of excited HAN come from the energy of the structure that corresponds to a vertical excitation from the minimum energy of E (Figure 2). According to the Franck−Condon principle, this is the point initially accessed upon a vertical photoexcitation. This point (not indicated in the figure) is located at 8.11 kcal/mol above the E* minimum and 2.62 and 0.58 kcal/mol above the TS_1* and TS_2*, respectively. Hence, the results predict that upon electronic excitation of E two channels may compete to dictate its spectroscopy and dynamics. One channel corresponds to the direct motion of the system in S_1 from the vibrationally highly excited E* to the potential of K* through (i) an intramolecular proton-transfer reaction coordinate and (ii) a possible subsequent motion from this well to that of KR* along a rotational coordinate. A comparable situation has been suggested to occur in other systems.[40,41] The opening of this channel depends on the excess energy at this level that possesses E* accessed upon a vertical transition. Beyond 8.11 kcal/mol, HAN has enough to surpass the first two energy barriers in S_1 (TS_1* and TS_2*) to produce K* and later to give the more stable KR* structure. The second operating channel, which has to compete with the former, involves intramolecular vibrational relaxation (IVR) in the gas phase or cooling (in condensed phase) processes of the vibrationally excited E*. This enol structure, brought at the bottom of the leftmost well in S_1 (Fig, 2B), has to relax to S_0 or to proceed to K* through a quantum-tunneling mechanism. Therefore, depending on the excitation energy and on the medium (gas or condensed phase), emission from E*, K*, or KR* might be observed. These expectations

are consistent with the experimental observation in molecular beam and in solution.[20,22,26]

As said above, the geometry of KR* (in S_1) is similar to that the TS found for the whole reaction of proton transfer and rotational motion in S_0. The possible connection between KR* and TS resembles the case of the PES for the isomerization of cyanine derivatives where the sink in the S_1 state (twisting of quinoline rings relative to each others) is coupled to a transition state in S_0.[42] It is also similar to the PES of the cis−trans isomerization in rhodopsin.[43−45] Therefore, relaxation processes from KR* to TS may occur, after which the molecule may return to either the original ground state conformation E or to the rotamer KR. The absence of a minimum energy at the ground state with a geometrical structure similar to that of KR* will not help in an efficient way the radiative relaxation to the ground state. Cheng and co-workers[21] reported that the lifetime of the excited keto tautomer (between 600 and 1200 ps) in the gas phase at room temperature decreases when the excess of energy excitation increases. They also showed the existence of an energy barrier for the conversion of E*, in agreement with our previous report on a molecular-beam experiment and with this work.[20] In solution, the lifetime of HAN ranges from 60 to 300 ps, depending on the viscosity of the solvent, and the emission quantum yield is around 10^{-3}.[26]

The dipole moment values of the involved structures in S_1 are not significantly different (E*(4.24 D), TS_1*(4.48 D), K*-(4.20 D), TS_2*(3.34 D), KR*(4.48D), TS_3*(3.90 D)). Therefore, we do not expect an appreciable solvent polarity effect on the stability of these structures. However, because of the involvement of a twisting motion, the emission properties of HAN are expected to be sensitive to the changes in temperature, viscosity, and caging of the medium. The potential energy curves for S_0 and S_1 predict a red-shifted emission of KR* when compared to that of K*. The twisting motion between K* and KR* will favor radiationless transitions. Therefore, the emission quantum yield of these species will be very low and dependent on the solvent viscosity. Again, these predictions have been experimentally observed by the Tobita group[22] and by us.[26] The twisting motion studied here from the point of view of theory for this relatively simple molecule might be relevant to the process exhibited by excited biological molecules such as the cis−trans isomerization process of rhodopsin.[43−45]

Finally, a striking difference between the dynamics of methyl salicylate (MS)[13] and that of HAN[20] is observed. The origin of this difference can be attributed to the difference in acidity of the OH group in the phenol and 1-naphthol parts and/or to the difference in energetic terms reflected in the stability of the proton-transfer tautomer relative to that of the enol one.[4] A distorted, single-minimum PES for MS has been suggested on the basis of experimental and theoretical works.[13,19] However, for HAN, this potential has several local minima as shown above, and it is not distorted like that of MS (Figure 2). Indeed, the excited keto and enol structures of HAN have almost similar energies. To overcome the barrier for the transfer, the excited HAN needs time to pass from the enol to the keto well, and this process can be controlled by modulating the in-plane and out-of-plane low-frequency modes of the H-bonded chelate ring. Thus, it seems that these related phenomena can be held responsible for the slow proton-transfer dynamics in excited HAN.

4. Conclusion

In summary, the ab initio calculations of the electronic structures of HAN show that upon electronic excitation to the S_1 state, the H-bonded structure is stabilized by about 2 kcal/mol relative to the ER−CO and ER−OH rotamers, where the H-bond is absent. The H-bond is stronger at S_1 than that found at the S_0 state. This is reflected in an increase in acidity and in basicity of the OH and $CO(CH_3)$ groups, respectively, and in a shortening of the O···O distance in E*. In-plane and out-of-plane vibrational motions of these partners in the H-bonded chelate ring might be the origin of the energy barrier for the proton-transfer reaction in E*. The existence of this barrier and the very small energy separation between E* and K* are in full agreement with the previous experimental results.[20] The very high activity of a bending mode (822 cm^{-1}) associated with the O−H out-of-plane motion in E* would explain the lack of emission signal in a jet-cooled molecular beam beyond ~900 cm^{-1} of excess energy at the S_1 state.[20] The produced K* tautomer may rotate to yield the KR* conformer, the most stable structure in the excited state. The presence of K* and KR* in S_1 may lead to a structured emission band and to the dependence of this on the viscosity/rigidity and the temperature of the medium. Its photophysics would also depend on the excess energy of excitation. These expectations accord with the experimental reports.[20−22,26]

The present results address fundamental issues for a better understanding of the dynamics and spectroscopy of molecules showing proton-transfer and twisting motion reactions. These movements are essential for the architecture, stability, function, and dynamics of macromolecules.[2,3,43−45]

Acknowledgment. Financial supports from the Ministry of Education and Science of Spain through projects 1FD1997-1658, PB98-0310, and PB98-0915 are gratefully acknowledged.

References and Notes

(1) Weller, A. Z. *Elektrochem.* **1956**, *60*, 1144.

(2) Caldin, E. F.; Gold, V. *Proton-Transfer Reactions*; Chapman and Hall: London, 1975. *Chem. Phys.* **1989**, 136. *J. Phys. Chem.* **1991**, *95*. Limbach, H.; Manz, J. (Eds.) Hydrogen Transfer: Experiment and Theory. *Ber. Bunsengens. Phys. Chem.* **1998**, *102*. Agmon, N.; Gutman, M. (Eds.) Proton Solvation and Proton Mobility. *Isr. J. Chem.* **1999**, *39*(3/4).

(3) Manz, J.; Wöste, L. (Eds.) *Femtochemistry: Ultrafast Dynamics of the Chemical Bond*; Word Scientific: Singapore, 1994. Zewail, A. H. *Femtosecond Chemistry*; VCH Publishers: Weinheim, 1995. Sundström, V. (Ed.) *Femtochemistry and Femtobiology*, *Nobel Symposium* 101; Imperial College Press: London, 1997.

(4) Douhal, A.; Lahmani, F.; Zewail, A. H. *Chem. Phys.* **1996**, *207*, 477 and references therein.

(5) Douhal, A.; Kim, S. K.; Zewail, A. H. *Nature* **1995**, *378*, 260.

(6) Chudoba, C.; Riedle, E.; Pfeiffer, M.; Elsaesser, T. *Chem. Phys. Lett.* **1996**, *263*, 622; Glasbeek, M. *Isr. J. Chem.* **1999**, *39* (3/4), 301 and references therein.

(7) Douhal, A. *Science* **1997**, *276*, 221.

(8) Smith, K. K.; Kaufmann, K. J. *J. Phys. Chem.* **1981**, *85*, 2895.

(9) Felker, P. M.; Lambert, W. R.; Zewail, A. H. *J. Chem. Phys.* **1982**, *77*, 1603.

(10) Helmbrook, L, Keny, J. E., Kohler, B. E., Scott, G. W. *J. Phys. Chem.* **1983**, *87*, 280.

(11) Toribio, F.; Catalán, J.; Acuña, A. U. *J. Phys. Chem.* **1983**, *87*, 817.

(12) Barbara, P. F.; Walsh, P. K.; Brus, L. E. *J. Phys. Chem.* **1989**, *93*, 29.

(13) Herek, J. L.; Pedersen, S.; Bañares, L.; Zewail, A. H. *J. Chem. Phys.* **1992**, *97*, 9046.

(14) Acuña, A. U.; Costela, A.; Muñoz, J. M. *J. Phys. Chem.* **1986**, *90*, 2870.

(15) Organero, J. A.; Douhal, A.; Santos, L.; Martínez-Ataz, E.; Guallar, V.; Moreno, M.; Lluch, J. M. *J. Phys. Chem. A.* **1999**, *103*, 5301. Guallar, V.; Douhal, A.; Moreno, M.; Lluch, J. M. *J. Phys. Chem.* **1999**, *103*, 6251.

(16) Naudorf, H.; Organer, J. A.; Douhal, A.; Kühn, O. *J. Chem. Phys.* **1999**, *110*, 11286.

(17) Vener, M. V.; Scheiner, S. *J. Phys. Chem.* **1995**, *99*, 642. Rovira, M. C.; Scheiner, S. *J. Phys. Chem.* **1995**, *99*, 9854. Scheiner, S.; Kar, T.; Çuma, M. *J. Phys. Chem. A* **1997**, *101*, 5901.

(18) Douhal, A.; Amat-Guerri, F.; Acuña, A. U. *Angew. Chem.* **1997**, *109*, 1586. *Angew. Chem., Int. Ed. Engl.* **1997**, *36*, 1514. Douhal, A. *Ber. Bunsen-Ges. Phys. Chem.* **1998**, *102*, 448. Mateo, C. R.; Douhal, A. *Proc. Natl. Acad. Sci. U.S.A.* **1998**, *95*, 7245. García-Ochoa, I.; Díez López, M.-A.; Viñas, M. H.; Santos, L.; Martínez-Ataz, E.; Amat-Guerri, F.; Douhal, A. *Chem. Eur. J.* **1999**, *5*, 897.

(19) Sobolewski, A. L. Domcke, W. *J. Phys. Chem. A*, **1999**, *103*, 4494. Sobolewski, A. L. Domcke, W. *Phys. Chem. Chem. Phys.* **1999**, *1*, 3065 and references therein.

(20) Douhal, A.; Lahmani, F.; Zehnacker-Rentien, A. *Chem. Phys.* **1993**, *178*, 493.

(21) Lu, C.; Hsieh, R.-M. R.; Lee, I.-R.; Cheng, P.-Y. *Chem. Phys. Lett.* **1999**, *310*, 103.

(22) Tobita, S.; Yamamoto, M.; Kurahayashi, N.; Tsukagoshi, R.; Nakamura, Y.; Shizuka, H. *J. Phys. Chem. A.* **1998**, *102*, 5206.

(23) Catalán, J., del Valle, J. C. *J. Am. Chem. Soc*. **1993**, *115*, 4321.

(24) Catalán, J.; Palomar, J.; G. de Paz, J. L. *Chem. Phys. Lett*. **1997**, *269*, 151.

(25) Organero, J. A.; et al. Submitted to *Chem. Phys. Lett*.

(26) Organero J. A.; et al. To be submitted.

(27) Guallar, V.; Moreno, M.; Lluch, J. M.; Douhal, A. *J. Phys. Chem*. **1996**, *100*, 19789.

(28) Douhal, A.; Guallar, V.; Moreno, M.; Lluch, J. M. *Chem. Phys. Lett.* **1996**, *256*, 370.

(29) Frisch, M. J.; Trucks, G. W.; Schlegel, H. B.; Gill, P. M. W.; Johnson, B. G.; Robb, M. A.; Cheeseman, J. R.; Keith, T. A.; Petersson, G. A.; Montgomery, J. A.; Raghavachari, K.; Al-Laham, M. A.; Zakrzewski, V. G.; Ortiz, J. V.; Foresman, J. B.; Cioslowski, J.; Stefanov, B. B.; Nanayakkara, A.; Challacombe, M.; Peng, C. Y.; Ayala, P. Y.; Chen, W.; Wong, M. W.; Andrés, J. L.; Replogle, E. S.; Gomperts, R.; Martin, R. L.; Fox, D. J.; Binkley, J. S.; Defrees, D. J.; Baker, J.; Stewart, J. P.; Head-Gordon, M.; Gonzalez, C.; Pople, J. A. *Gaussian 94*; Gaussian Inc.: Pittsburgh, PA, 1995.

(30) Frisch, M. J.; Trucks, G. W.; Schlegel, H. B.; Scuseria, G. E.; Robb, M. A.; Cheeseman, J. R.; Zakrzewski, V. G.; Montgomery, J. A.; Stratmann, R. E., Burant, J. C.; Dapprich, S., Millam, J. M.; Daniels, A. D.; Kudin, K. N.; Strain, M. C.; Farkas, O.; Tomasi, J.; Barone, V.; Cossi, M.; Cammi, R.; Mennuci, B.; Pomelli, C.; Adamo, C.; Clifford, S.; Ochterski, J.; Petersson, G. A.; Ayala, P. Y.; Cui, Q.; Morokuma, K.; Malick, D. K.; Rabuck, A. D.; Raghavachari, K.; Foresman, J. B.; Cioslowski, J.; Ortiz, J. V.; Stefanov, B. B.; Liu, G.; Liashenko, A.; Piskorz, P.; Komaromi, I.; Gomperts, R.; Martin, R. L.; Fox, D.J; Keith, T.; Al-Laham, M. A.; Peng, C. Y.;. Nanayakkara, A.; Gonzalez, C.; Challacombe, M.; Gill, P. M. W.; Johnson, B. G.; Chen, W.; Wong, M. W.; Andrés, J. L.; Head-Gordon, M.; Replogle, E. S.; Pople, J. A. *Gaussian 98*; Gaussian Inc.: Pittsburgh, PA, 1998.

(31) Foresman, J. B.; Head-Gordon, M.; Pople, J. A.; Frisch, M. J. *J. Phys. Chem*. **1992**, *96*, 135.

(32) Møller, C.; Plesset, M. S. *Phys. Rev*. **1934**, *46*, 618.

(33) Ditchfield, R.; Hehre, W. J.; Pople, J. A. *J. Chem. Phys*. **1971**, *54*, 724; **1972**, *56*, 2257. Hariharan, P. C.; Pople, J. A. *Mol. Phys*. **1974**, *27*, 209. Gordon, M. S. *Chem. Phys. Lett.* **1980**, *76*, 163; Clark, T.; Chandrasekar, J.; Spitznagel, G. W.; Schleyer, P. v. R. *J. Comput. Chem*. **1983**, *4*, 294.

(34) Hehre, W. J.; Radom, R.; Schleyer, P.v. R.; Pople, J. A. *Ab Initio Molecular Orbital Theory*, J. Wiley & Sons: New York, 1986.

(35) Syage, A. *J. Phys. Chem*. **1993**, *97*, 12523.

(36) Smulevich, G.; Amirav, A.; Even, E.; Jortner, J. *Chem. Phys*. **1982**, *73*, 1.

(37) Ernsting, N. P. *J. Phys. Chem*. **1985**, *89*, 4932.

(38) Douhal, A.; Lahmani, F.; Zehnacker-Rentien, A.; Amat-Guerri, F. *J. Phys. Chem*. **1994**, *98*, 12198.

(39) Catalán, J.; del Valle, J. C.; Palomar, J.; Díaz, C.; de Paz, J. L. G. *J. Phys. Chem. A* **1999**, *103*, 10921.

(40) Fiebig, T.; Chachisvilis, M.; Manger, M.; Zewail, A. H.; Douhal, A.; Garcia-Ochoa, I.; de La Hoz Ayuso, A. *J. Phys. Chem. A.* **1999**, *103*, 7419.

(41) Douhal, A.; Fiebig, T.; Chachisvilis, M.; Zewail, A. H. *J. Phys. Chem. A.* **1998**, *102*, 1657.

(42) Alvarez, J.-L.; Yartsev, A.; Aberg, U.; Akesson, E.; Sundström, V. *J. Phys. Chem. B* **1998**, *102*, 7651 and references therein.

(43) Wang, Q.; Schoenlein, R. W.; Peteanu, L. A.; Mathies, R. A.; Shank, C. V. *Science* **1994**, *266*, 422.

(44) Logunov, S. L.; Song, L.; El-Sayed, M. A. *J. Phys. Chem*. **1996**, *100*, 18586.

(45) Song, L.; El-Sayed, M. A. *J. Am. Chem. Soc*. **1998**, *120*, 8889. Hahn, S.; Stock, G. *J. Phys. Chem. B.* **2000**, *104*, 1146 and references therein.